Dinuclear Nickel Complexes as Catalysts for Electrochemical Reduction of Carbon Dioxide

Eugenio Simón-Manso and Clifford P. Kubiak*

Department of Chemistry and Biochemistry, University of California−San Diego, 9500 Gilman Drive, La Jolla, California 92093-0358

Received July 14, 2004

Dinuclear Ni(0) complexes $[Ni_2(\mu\text{-dppa})_2(\mu\text{-CNR})(CNR)_2]$ (R = Me (**1**), n-Bu (**2**), and 2,6-$Me_2C_6H_3$ (**3**); dppa = bis(diphenylphosphine)amine) were synthesized in good yields by reacting $Ni(COD)_2$ with dppa and the corresponding isocyanide. The X-ray structure of complex **1** is reported. The electrochemistry and spectroelectrochemistry of each complex are also reported. Complex **2** exhibits an irreversible 1 e^- reduction at −0.99 V vs ferrocene in its cyclic voltammogram. When the cyclic voltametry was performed in the presence of CO_2, a substantial current enhancement was observed for the reduction wave. Spectroelectrochemical as well as isotope labeling studies show that **2** is singly reduced to a radical anion species that is reactive toward CO_2, yielding the disproportionation products CO and CO_3^{2-}. In the presence of H^+ donors (residual water), reduction of CO_2 to formate is a competing process.

Introduction

Carbon dioxide is the end product of many industrial and biological processes; however, only plants can effectively regenerate useful products from it. The electrocatalytic reduction of carbon dioxide to organic molecules has drawn the attention of many research groups.[1−5] Bis(diphenylphosphine)methane (dppm) is frequently used as a supporting ligand in transition metal complexes that show activity toward the reduction of CO_2.[1] Polynuclear complexes containing dppm have been shown to react with CO_2 photochemically,[2] electrochemically,[3] and chemically.[4] Similar disphosphines such as bis(diphenylphosphine)amine (dppa) have received less attention in the development of polynuclear complexes.[2] Recently, dinuclear[5] and trinuclear[6] nickel complexes with dppa as a supporting ligand have been reported. In our continuing studies of carbon dioxide activation using polynuclear transition metal complexes, we describe the synthesis, characterization, and electrocatalytic properties of dinuclear nickel complexes $[Ni_2(\mu\text{-dppa})_2(\mu\text{-CNR})(CNR)_2]$ (R = Me, n-Bu, xylyl) with bridging dppa ligands. In addition, the X-ray structure of complex $[Ni_2(\mu\text{-dppa})_2(\mu\text{-CNCH}_3)(CNCH_3)_2]$, **1**, is reported.

* Corresponding author. Tel: 858-822-2665. Fax: 858-534-5383. E-mail: ckubiak@ucsd.edu.

Experimental Section

Materials and Physical Measurements. All manipulations were performed under a nitrogen atmosphere using a glovebox or Schlenk techniques. $Ni(COD)_2$, MeNC, and the ligand $NH(PPh_2)_2$ (dppa) were synthesized according to literature procedures.[7,8] CN(n-Bu) and CN(2,6-$Me_2C_6H_3$), CN(2,6-$Me_2C_6H_3$) = CNxylyl, were purchased from Aldrich and used without further purification. Isotopically labeled chemicals ($H_2{}^{18}O$, $^{13}CO_2$) were purchased from Cambridge Isotope Laboratories, Inc. The carbon dioxide concentration in acetonitrile solutions was measured using an IR method reported previously.[9] Solvents were purchased from Fisher Scientific and purified by passing through aluminum oxide columns under nitrogen pressure. ^1H and ^{31}P NMR spectra were obtained using a Varian Mercury 400 spectrometer, and ^{31}P NMR spectra were referenced with respect to external 85% H_3PO_4. Elemental analyses were performed by Midwest Microlab. KBr FTIR spectra were recorded using Mattson (Research Series 1) and Bruker (Equinox 55) spectrophotometers. Cyclic voltammetric (CV) measurements were carried out using a BAS-CV-50w electrochemical workstation. The working electrodes were a platinum disk (CV) or a platinum mesh (coulometry). The supporting electrolyte was tetrabutylammonium hexafluorophosphate ($TBA^+PF_6^-$). All potentials are reported with respect to a ferrocene/ferrocenium (Fc/Fc^+) reference electrode. The spectroelectrochemical (SEC) measurements were performed in a cell constructed by our group and reported previously.[10] Bulk electrolysis at a potential of −1.3 V and temperature of −70 °C was used to generate the reduced species. The electrochemical cell was held in a specially constructed brass circulation unit inside the drybox and connected to an outside refrigerated circulating bath. The EPR experiments were performed using a Bruker continuous

(1) Bhattacharyya, P.; Woollins, D. J. *Polyhedron* **1995**, 3367−3388.
(2) Morgenstern, D. A.; Wittrig, R. E.; Fanwick, P. E.; Kubiak, C. P. *J. Am. Chem. Soc.* **1993**, *115*, 6470−6471.
(3) Morgenstern, D. A.; Ferrence, G. M.; Washington, J.; Henderson, J. I.; Rosenhein, L.; Heise, J. D.; Fanwick, P. E.; Kubiak, C. P. *J. Am. Chem. Soc.* **1996**, *118*, 2198−2207.
(4) DeLaet, D. L.; Fanwick, P. E.; Kubiak, C. P. *J. Am. Chem. Soc., Chem. Commun.* **1987**, 1412−1413.
(5) Simon-Manso, E.; Valderrama, M.; Arancibia, V.; Simon-Manso, Y.; Boys, D. *Inorg. Chem.* **2000**, *39*, 1650−1654.
(6) Simon-Manso, E.; Gantzel, P.; Kubiak, C. P. *Polyhedron* **2003**, *22*, 1641−1644.
(7) Schunn, R. A.; Ittel, S. D.; Cushing, M. A. *Inorg. Synth.* **1974**, *25*, 95−97.
(8) Jackson, H. L.; McKusick, B. C. *Organic Syntheses*; John Wiley: New York, 1955; Vol. 35.
(9) Haines, R. J.; Wittrig, R. E.; Kubiak, C. P. *Inorg. Chem.* **1994**, *33*, 4723−4728.
(10) Zavarine, I. S.; Kubiak, C. P. *J. Electroanal. Chem.* **2001**, *495*, 106−109.

10.1021/om0494723 CCC: $30.25
Publication on Web 11/24/2004

Table 1. Crystal Data and Data Collection Parameters for 1

formula	$C_{54}H_{51}N_5P_4Ni_2$
fw	1010.28
space group	$P\bar{1}$
cryst syst	triclinic
a, Å	12.8286(10)
b, Å	13.5102(11)
c, Å	14.9130(12)
α, deg	81.9030(10)
β, deg	85.7970(10)
γ, deg	74.0030(10)
V, Å^3	2458.2(3)
Z	2
d_{calc}, g cm^{-3}	1.366
cryst dimens, mm	0.2 × 0.2 × 0.1
temperature, K	100(2)
F_{000}	1052
GOF	0.964
final R indices [$I > 2\sigma(I)$], R1	0.0531

wave E500 spectrometer of the Elexsys Series at 5 K in frozen THF. Density functional calculations (DFT) were done using a hybrid functional developed by Becke[11] along with Perdew and Wang correlation,[12] using the LANL2DZ basis set (b3pw91/LanL2DZ) as implemented in Gaussian98.[13]

[Ni$_2$(μ_2-dppa)$_2$(μ_2-CNMe)(CNMe)$_2$], 1. To a solution of dppa (286 mg, 2.54 mmol) was added Ni(COD)$_2$ (700 mg, 2.54 mmol) dissolved in 20 mL of toluene. The solution was stirred for 5 min, and then 2.4 mL of a THF solution containing CNMe (7.2 mmol, 10% molar excess) was added. The solution was stirred for 1 h, and then the volume was reduced to 5 mL under vacuum. The product was precipitated as a red solid upon addition of excess pentane. The product was collected by filtration and washed with several portions of pentane and then dried under vacuum. Anal. Calcd for $C_{54}H_{51}N_5P_4Ni_2$: C, 64.14; H, 5.04. Found: C, 64.25; H, 5.39. ^{31}P NMR (toluene-d_8): 69.5 (s). ^{1}H NMR (toluene-d_8): 2.95 (s, 6H, Me), 2.12 (s, 3H, Me). IR (KBr) ν(NC): 2080, 1723 cm^{-1}.

[Ni$_2$(μ_2-dppa)$_2$(μ_2-CNR)(CNR)$_2$] (n-Bu, 2; xylyl, 3). Complexes **2** and **3** were synthesized using the same procedure as for complex **1**, but with an isocyanide/Ni(COD)$_2$ ratio of 3:2.

Complex 2. Anal. Calcd for $C_{63}H_{69}N_5P_4Ni_2$: C, 66.53; H, 6.07. Found: C, 66.25; H, 6.23. ^{31}P NMR (benzene-d_6): 68.58 (s). ^{1}H NMR (benzene-d_6): 3.5 (m, 4H, CH_2), 2.75 (m, 8H, CH_2), 1.8 (m, 9H, CH_3). IR (KBr) ν(NC): 2074, 1723, 1710 cm^{-1}.

Complex 3. Anal. Calcd for $C_{75}H_{69}N_5P_4Ni_2$: C, 70.29; H, 5.39. Found: C, 70.38; H, 5.26. ^{31}P NMR (benzene-d_6): 69.5 (s). ^{1}H NMR (benzene-d_6): 2.478 (s, 6H, Me), 1.907 (s, 12H, Me), 6.6 (m, Ph), 6.87 (m, Ph), 7.15 (m, Ph), 7.35 (m, Ph), 7.79 (br, Ph). IR (KBr) ν(NC): 2038, 1833, 1745 cm^{-1}.

X-ray Experimental. Intensity data were collected on a Nonius Kappa CCD diffractometer using graphite-monochromated Mo Kα ($\lambda = 0.71073$ Å) radiation in the Wyckoff ω scan mode. The structures were solved by direct methods, and all of the non-hydrogen atoms were refined with anisotropic thermal parameters. Refinement was by full-matrix least-squares methods on F^2. Calculations were performed using the program SHELXTL-PC. Phenyl rings were treated as idealized D_{6h} symmetric rings with d(C−C) = 1.395 Å and ∠(C−C−C) = 120°. Crystal data and details of measurements and refinements are summarized in Table 1.

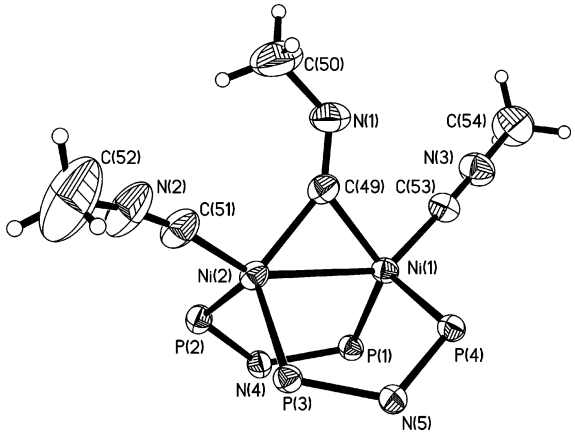

Figure 1. ORTEP diagram (thermal ellipsoid 50%) for complex [Ni$_2$(μ_2-dppa)$_2$(CNCH$_3$)$_2$(μ-CNCH$_3$)], **1**. The phenyl rings are omitted for clarity. Selected bond length (Å) and angles (deg): Ni(1)−Ni(2), 2.5174(9); Ni(1)−P(1), 2.1694(14); Ni(2)−P(2), 2.1876(15); Ni(1)−C(49), 1.905(5); Ni(2)−C(49), 1.914(5); Ni(1)−C(53), 1.822(5); Ni(2)−C(51), 1.803(6); P(3)−N(5), 1.706(4); P(4)−N(5), 1.710(4); C(49)−N(1), 1.220(7); N(1)−C(50), 1.446(8); C(53)−N(3), 1.146(7); N(3)−C(54), 1.425(8); C(51)−N(2), 1.163(8); N(2)−C(52), 1.423(10). P(1)−Ni(1)−P(4), 113.02(5); P(2)−Ni(2)−P(3), 110.04(6); C(53)−Ni(1)−C(49), 95.0(2); C(51)−Ni(2)−C(49), 101.8(3); C(53)−Ni(1)−Ni(2), 141.87(17); C(51)−Ni(2)−Ni(1), 148.3(2); P(3)−N(5)−P(4), 115.8(2); P(2)−N(4)−P(1), 117.3(2).

CIF file for complex **1** has been deposited with the Cambridge Crystallographic Database (Deposition Number 212125). These data can be obtained free of charge via www.ccdc.cam.ac.uk/conts/retrieving.html (or from the CCDC, 12 Union Road, Cambridge CB2 1EZ, UK; fax: +44 1223 336033; e-mail: deposit@ccdc.cam.ac.uk).

Results and Discussion

Synthesis. Dppa reacts with Ni(COD)$_2$ in the presence of aryl and alkyl isocyanides (CNR) to give the dinuclear nickel complexes Ni$_2$(μ_2-dppa)$_2$(μ_2-CNR)(CNR)$_2$ in good yield. These complexes are isoelectronic and similar overall to dppm-bridged dimers reported earlier.[14−16] All of the complexes are air sensitive. They were fully characterized by ^{31}P and ^{1}H NMR, elemental analysis, and IR. Like the dppm analogues, the different isocyanide ligands do not affect the ^{31}P NMR chemical shift (69 ± 1 ppm) significantly, indicating that the orbitals involving the phosphorus nickel bonds do not interact appreciably with those involved in nickel−isocyanide bonding.

Molecular Structure of Complex 1. The structure of **1**, Figure 1, appears similar to its dppm analogue Ni$_2$(μ_2-dppm)$_2$(μ_2-CNCH$_3$)(CNCH$_3$)$_2$.[17] Complex **1** has a "W-frame" or "cradle" type structure with two μ-bridging dppa ligands between the nickel atoms and three isocyanide ligands, of which two are terminal and one is bridging to the two metal centers. Crystal data and data collection parameters for complex **1** are summarized in Table 1.

(11) Becke, A. D. *J. Chem. Phys.* **1993**, *98*, 5648.
(12) Perdew, W.; Perdew, J. P.; Wang, Y. *Phys. Rev. B* **1992**, *45*, 13244.
(13) Frisch, M. J.; Trucks, G. W.; Schlegal, H. B.; Gill, P. M. W.; Johnson, B. G.; Robb, M. A.; Cheesman, J. R.; Keith, T.; Petersson, G. A.; Montgomery, J. A.; Raghavachari, K.; Al-Laham, M. A.; Zakrzewski, V. G.; Ortiz, J. V.; Foreman, J. B.; Peng, C. Y.; Ayala, P. Y.; Chen, W.; Wong, M. W.; Andres, J. L.; Replogle, E. S.; Comperts, R.; Martin, R. L.; Fox, D. J.; Binkley, J. S.; Defrees, D. J.; Baker, J.; Strwart, J. P.; Head-Gordon, M.; Gonzalez, C.; Pople, J. A. *Gaussian 94*, revision B.3; Gaussian, Inc.: Pittsburgh, PA, 1995.
(14) Ratliff, K. S.; DeLaet, D. L.; Gao, J.; Fanwick, P. E.; Kubiak, C. P. *Inorg. Chem.* **1990**, *29*, 4022.
(15) DeLaet, D. L.; Del Rosario, R.; Fanwick, P. E.; Kubiak, C. P. *J. Am. Chem. Soc.* **1987**, *109*, 754−758.
(16) Gong, J.; Kubiak, C. P. Ph.D. Thesis, Purdue University, 1990; p 181.
(17) DeLaet, D. L.; Fanwick, P. E.; Kubiak, C. P. *Organometallics* **1986**, *5*, 1807−1811.

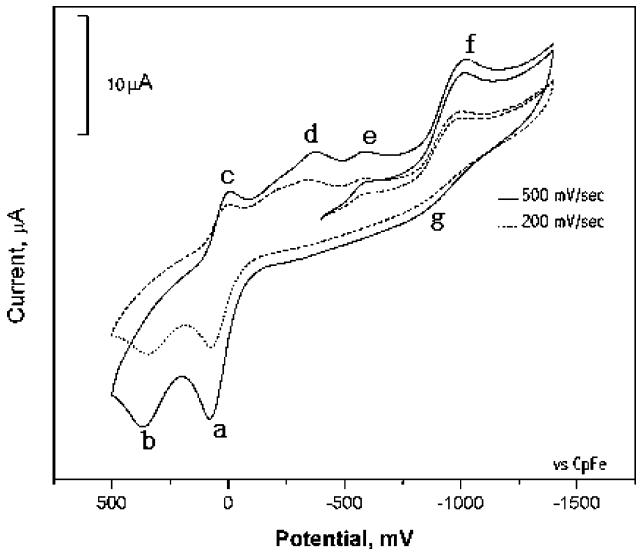

Figure 2. CV for complex **2** at two different scan rates (200, 500 mV/s).

The Ni−Ni (2.5174(9) Å) and Ni−P_{av} bond lengths (2.1810(14) Å) in **1** are slightly shorter than those in the dppm analogue (Ni−Ni, 2.572(1) Å; Ni−P_{av}, 2.205(8) Å).[17] In the case of the dppa dimer, stronger metal phosphorus interactions are understandable in terms of a more accessible σ^* orbital of the phosphine ligand. This is due to the presence of more electronegative nitrogen, directly attached to the phosphorus atom, lowering the energy of the σ^* orbital and making it a better acceptor for dπ electron density from the metal centers.[18]

The bridging phosphines have little effect on the μ-isocyanide bond lengths (**1**, 1.220(7) Å; dppm analogue, 1.239(7) Å), which is reflected in IR spectroscopic data (**1**, 1723 cm^{-1}; dppm analogue 1715 cm^{-1}). The nickel−carbon bond lengths are also similar in both complexes (Ni−C_{term}: **1**, 1.803(6), 1.822(5) Å vs 1.799(7), 1.796(6) Å; Ni−C_{bridge}: **1**, 1.905(5), 1.914(5) Å vs 1.903(6), 1.929(6) Å).

Electrochemical Studies under N_2. The cyclic voltammograms of complex **2** in acetonitrile solution at two different scan rates are shown in Figure 2. The positive scans show one quasi-reversible oxidation peak at 0.07 V (a) and a second irreversible oxidation peak at 0.345 V (b). The small reduction evident at 0.01 (peak c) corresponds to products of oxidation a. Reductions at −0.3 and −0.6 V (peaks d,e) appeared as a result of oxidations a and b, respectively. Chemical oxidation of the isoelectronic dppm analogue compounds led to formation of complexes having intact dinuclear mixed valence frameworks $[Ni_2]^+$ and $[Ni_2]^{2+}$.[19]

The major structural change in the $[Ni_2]^+$ complex is an elongation of the CN bond at the bridging position. In the case of the $[Ni_2]^{2+}$complex, internal disproportionation of a Ni(I)−Ni(I) species occurs, leading to formation of mixed valence [Ni(II)−Ni(0)] complexes.[19] Similar structural changes are expected in the dppa dinuclear compounds upon oxidation. These structural rearrangements, which give rise to more stable oxidized species, can explain the generally irreversible nature of the electrochemical oxidations (reduction peaks d and e after oxidations a and b). The scan toward negative potentials shows an irreversible reduction at −0.99 V (peak f). Peak g corresponds to reoxidation of the organonickel radical anion, expected by reduction f. It is also evident that at room temperature these species are not sufficiently structurally stable for their reoxidation to be seen in the reverse scan, even at a high scan rate (500 mV s^{-1}).

Peak f shifts cathodically by 23 mV when the scan rate is increased from 200 to 500 mV s^{-1}. The CVs recorded for complexes **1** and **3** in THF (complexes **1** and **3** are less soluble in acetonitrile) have the same overall shape with little variation in their redox potentials. The reduction peak at ca. −1.0 V, in the case of complex **2** (peak f, Figure 2), is quite small for complexes **1** and **3**. This suggests either sluggish kinetics in the reduction of these complexes or an increased instability of the electrochemically reduced species. This may be explained because of greater reactivity of the radical anions of these complexes in THF solvent.

Spectroelectrochemical (SEC) Studies. A IR SEC cell[11] was employed to investigate the electronic and structural changes when **2** is reduced or oxidized. Figure 3a−c shows the IR−SEC response in the ν(NC) region at −1.3, 0.0, and +0.2 V vs Ag wire at −35 °C, respectively. Upon reduction at −1.3 V, the bands at 2086 and 1710 cm^{-1}, which correspond to the terminal and bridging isocyanides, respectively, decreased and new bands grew in at 2050 and 1676 cm^{-1} with clear isosbestic points at 2069 and 1693 cm^{-1}. The simultaneous shift of both bands by 36 to 34 cm^{-1} to lower energy is consistent with electron density being added to the $\pi^*_{C=N}$ orbitals while maintaining the overall "W-frame" structure of the dimer.

Ligand-based reduction is consistent with theoretical calculations involving complex **2**, which are discussed later. Reoxidation at −0.35 V gave the starting neutral species $\mathbf{2}^0$. The reversible structural changes that accompany ET (peak f, Figure 2) and the cathodic shift of f with an increase in scan rate strongly suggest an E_{irrev} mechanism for the reduction process f.[20]

When the sample was oxidized at 0 V (peak a in CV), the bands at 2086 and 1710 cm^{-1}, which correspond to the neutral species, disappeared, and a new band at 2134 cm^{-1} grew in, suggesting that a significant amount of charge has been removed from the CN bridge after the 1 e^- oxidation occurs (Figure 3b, $\mathbf{2}^+$ species). Oxidation of the neutral species $\mathbf{2}^0$ at more positive potentials (+0.20 V) is accompanied by a rapid appearance and disappearance of species $\mathbf{2}^+$ (2134 cm^{-1}), followed by new bands at 2169 and 2024 cm^{-1} (Figure 3c). A clean isosbestic point at 2152 cm^{-1} links this transformation. These results are consistent with an internal redox disproportionation reaction of the two Ni(I)−Ni(I) centers to a Ni(II)−Ni(0) formulation with one of the isocyanides bonded to a Ni(II) (2169 cm^{-1}) and the other to a Ni(0) center (2024 cm^{-1}). Similar redox disproportionations are observed in other nickel dimers upon 2 e^- oxidations.[19] These changes are chemically reversible, and the neutral $\mathbf{2}^0$ species can be

(18) Orpen, A. G. *Chem. Commun.* **1985**, 1310.
(19) Ferrence, G. M.; Simón-Manso, E.; Breedlove, B. K.; Meeuwenberg, L.; Kubiak, C. P. *Inorg. Chem.* **2004**, *43*, 1071−1081.
(20) Astruc, D. *Electron Transfer and Radical Processes in Transition-Metal Chemistry*; Wiley-VCH: New York, 1995.

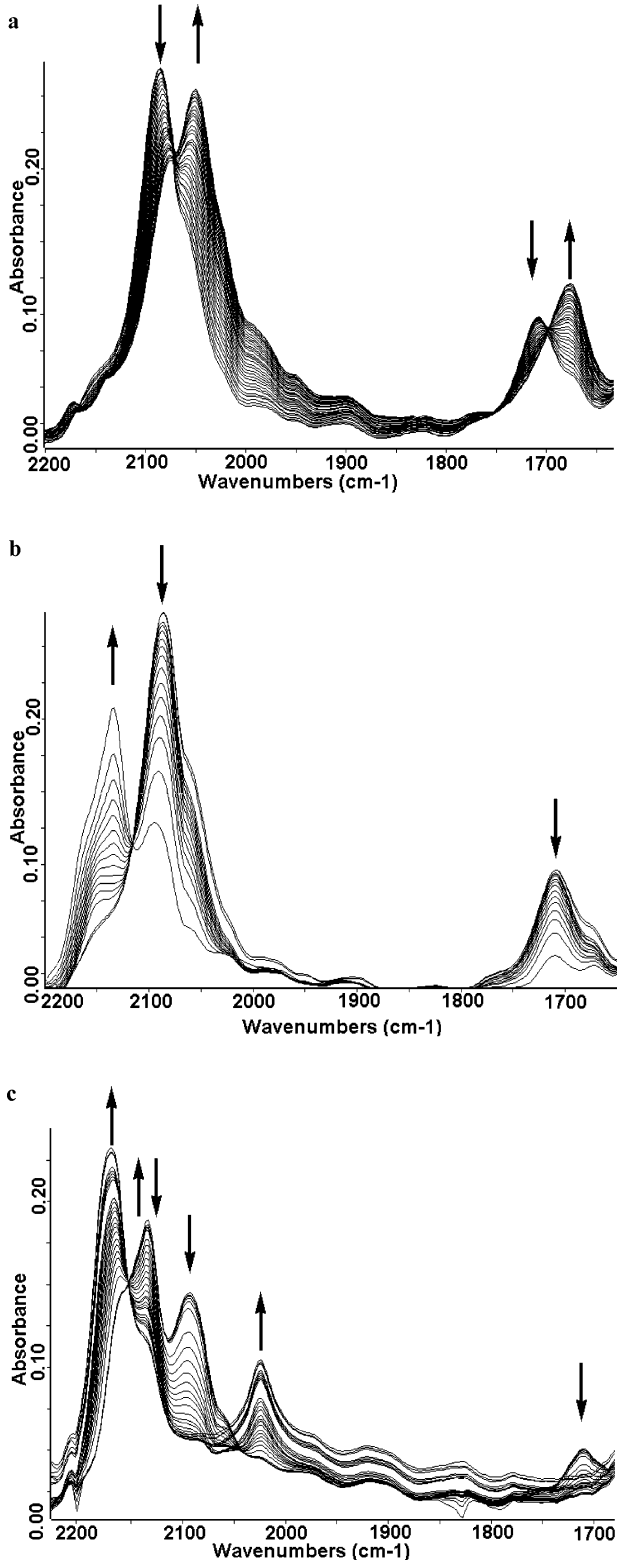

Figure 3. (a) Observed changes in the IR (2200−1600 cm^{-1}) for complex **2** with an applied potential of −1.3 V vs Ag pseudoreference electrode. (b) Observed changes in the IR (2500−1600 cm^{-1}) for complex **2** at 0.0 V. (c) Observed changes in the IR (2500−1600 cm^{-1}) for complex **2** at +0.2 V.

regenerated by electrolysis at −0.7 V. The SEC results are summarized in Scheme 1.

To obtain more information about the nature of the species formed during the electrochemical reduction (peak f in Figure 2), an EPR experiment was performed.

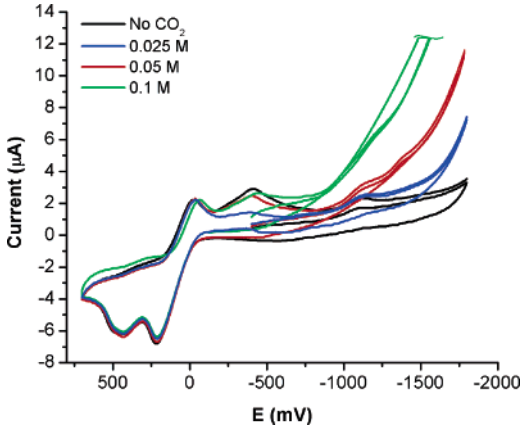

Figure 4. Current enhancement of the reduction wave observed in the CV (scan rate = 200 mV/s) for complex **2** at three different [CO_2] concentrations (0.0025, 0.050, and 0.100 M) in acetonitrile solution.

Because the reduced species is unstable at −35 °C, bulk electrolysis was performed at −70 °C using a special electrochemical setup (see Materials and Physical Measurements section). After electrolysis, the sample was transferred to an EPR tube and kept in liquid nitrogen for EPR evaluation. The EPR signal in frozen THF solution at 4 K (see Supporting Information for spectrum) is broad and has an average *g*-value of 2.05. Although the EPR spectrum is not sufficiently resolved to make definitive conclusions about the structure of the reduced species, the fact that upon reduction the generated species is not EPR silent tells us about the radical nature of this electrochemically generated species. Ligand-based reduction is in agreement with IR spectroelectrochemical results and the ligand-centered character of the LUMO in the isoelectronic $Ni_2(dppa)_2(CO)_3$ complex,[5] as well as the calculated LUMO for complex **1** (see below). Also, the broad appearance of the EPR spectrum could be related to an unpaired electron occupying a degenerate LUMO (see theoretical calculations below), where fast spin relaxation is expected.

Cyclic Voltammetry in the Presence of CO_2. The cyclic voltammograms of complex **2** in the presence of concentrations of CO_2 (0.0025, 0.050, and 0.100 M),[9] Figure 4, showed a large [CO_2]-dependent increase in current of the cathodic wave at −1.0 V while the oxidation waves remained unchanged.

The current increases with increasing CO_2 concentrations indicate an electrochemical process that is bimolecular and directly involves CO_2. The simplest mechanism is represented by eqs 1 and 2.

$$[Ni_2]^0 + e^- \rightharpoonup [Ni_2]^{-\bullet} \quad (1)$$

$$[Ni_2]^{-\bullet} + CO_2 \xrightarrow{k'} [Ni_2]^0 + CO_2^{-\bullet} \quad (2)$$

After purging with argon, the cyclic voltammogram returns to its original shape. According to eqs 3 and 4, derived by Saveant and Vianello,[21,22] the limiting current for a catalytic reaction with reversible charge

(21) Nicholson, R. S.; Irving, S. *Anal. Chem.* **1964**, *36*, 706−723.
(22) Saveant, J. M.; Vianello, E. *Advances in Polarography*; Pergamon Press: New York, 1960; Vol. 1.

Scheme 1

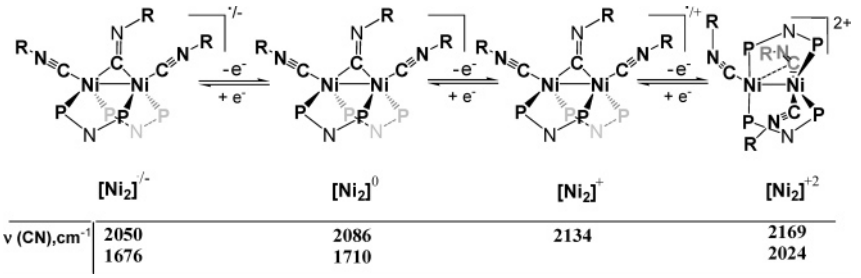

transfer is proportional to the rate constant and independent of the scan rate.

$$i = nFACo\sqrt{Dk_f} \quad (3)$$

$$k_f = k'[CO_2] \quad (4)$$

where i is the observed cathodic current at −1.3 V, n is the number of transferred electrons during the electrochemical reaction, A is the area of the working electrode, F is the Faraday constant, Co is the concentration of the $[Ni_2]^0$ species in the bulk, D is the diffusion coefficient, calculated from the CV data,[23] and k' is the rate constant for the homogeneous electron transfer reaction between the electrochemically reduced organonickel radical and CO_2.

For a large value of k_f (eq 3) and very cathodic potentials, no wave should be observed. In our system, the cyclic voltammogram in the cathodic region shows no differences at scan rates between 20 and 500 mV s^{-1}, adding support to the mechanism proposed above (eqs 1 and 2). The rate constant k' for the bimolecular reaction eq 2, evaluated according to eqs 3 and 4 from the CV data, equals 29.0 M^{-1} s^{-1}. This is a significantly higher value, compared to the previously studied nickel cluster radicals $[Ni_3(\mu_2\text{-dppm})_3(\mu_3\text{-L})(\mu_3\text{-I})]$ (L = CNR, R = CH_3, i-C_3H_7, C_6H_{11}, $CH_2C_6H_5$, t-C_4H_9, 2,6-$Me_2C_6H_3$; L = CO), where the rate constants for the rate-limiting step in the reduction of CO_2 by the clusters, k_{CO_2} (M^{-1} s^{-1}), were estimated to range between 1.6 and 0.01, having the lower values for the more sterically hindered clusters.[24]

It is interesting to note that the isoelectronic complex $[Ni_2(\mu_2\text{-dppm})_2(\mu_2\text{-CNMe})(CNMe)_2]$ has two quasi-reversible oxidation peaks. In the presence of CO_2, the *second* cathodic wave shows current enhancement in the cyclic voltammogram, which was interpreted in terms of an EC mechanism, resulting from an irreversible chemical reaction with CO_2 to give a $[Ni_2(\mu_2\text{-dppm})_2(\mu_2\text{-CNMe})(CNMe)_2]\cdot CO_2$ complex, where the C and O atoms of CO_2 and C and N atoms of the bridging isocyanide form a four-membered ring.[17] The rupture of the four-membered ring of this intermediate leads to the formation of carbonyl complex $[Ni_2(\mu_2\text{-dppm})_2(\mu_2\text{-CO})(CO)_2]$, confirmed by isotopic labeling studies.

IR SEC Results in the Presence of CO_2. A 0.1 mM solution of complex **2** in acetonitrile (TBAP 0.1 M) with CO_2 was injected into the IR SEC cell. Large currents (~5 mA) were observed when the solution was electrolyzed at −1.3 V vs a silver pseudoreference electrode. Figure 5 shows that the spectral changes in the ν(NC) region were very different from those observed upon reduction of complex **2** in argon-saturated CH_3CN solution at this potential (Figure 3a).

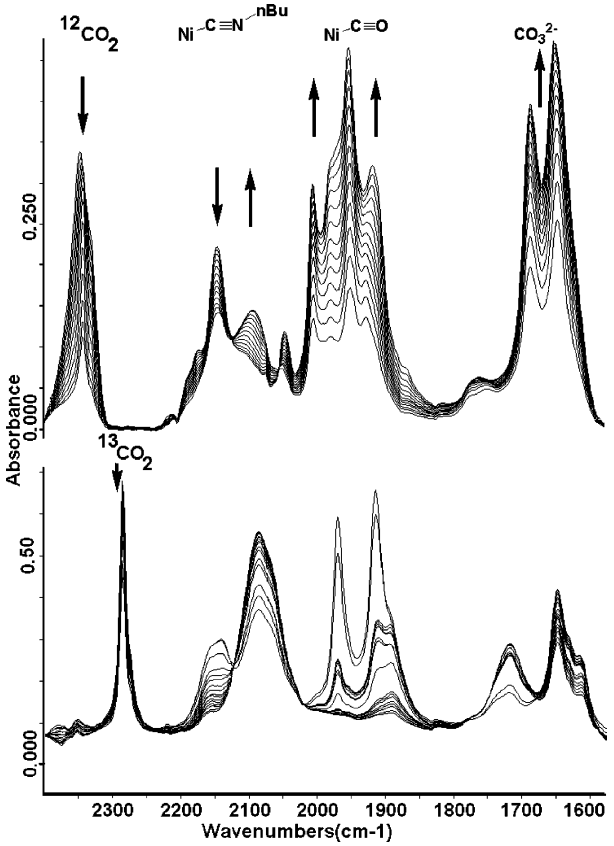

Figure 5. Observed changes in the IR (2500−1600 cm^{-1}) spectrum during the bulk electrolysis at −1.3 V of $[Ni_2(\mu_2\text{-dppa})_2(\mu_2\text{-n-BuNC})(\text{n-BuNC})_2]$ (**2**) in the presence of CO_2 (SEC) ($^{12}CO_2$, top; $^{13}CO_2$, bottom).

The ν(NC) band at 2086 cm^{-1}, corresponding to terminally coordinated isocyanides, decreased slightly in intensity, and new bands at 2004, 1980, 1950, 1926, 1685, and 1650 cm^{-1} were observed. Toward the end of the electrolysis, the bands around 2000 cm^{-1} are slightly shifted, with the most intense absorptions at 2004, 1953, 1916, and 1868 cm^{-1}.

The two bands at 1685 and 1650 cm^{-1} are similar to the bands reported for carbonate anion in acetonitrile solution.[25] The bands at 2004, 1980, 1950, and 1926 cm^{-1} are similar to those reported for terminal and

(23) Morikita, T.; Yamamoto, T. *J. Organomet. Chem.* **2001**, *637−639*, 809−812.

(24) Wittrig, R. E.; Ferrence, G. M.; Washington, J.; Kubiak, C. P. *Inorg. Chim. Acta* **1998**, *270*, 111−117.

(25) Cheng, S. C.; Blaine, C. A.; Hill, M. G.; Mann, K. R. *Inorg. Chem.* **1996**, *35*, 7704−7708.

Scheme 2

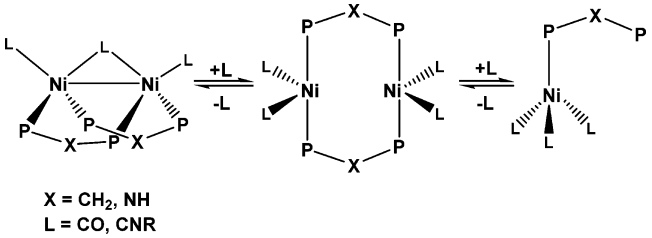

bridging carbonyls in dppm[26] and dppa[5] nickel dimers. These results suggest that the CO_2 reductively disproportionates into CO and CO_3^{2-} and that the CO is "trapped" by the nickel catalyst, explaining why no bands in the region of free CO (2138 cm^{-1}) grow in during the electrolysis. The ready and reversible uptake of CO by $[Ni_2(\mu_2\text{-dppm})_2(\mu_2\text{-CO})(CO)_2]$ and $[Ni_2(\mu_2\text{-dppa})_2(\mu_2\text{-CO})(CO)_2]$ was reported.[5,26] An equilibrium like the one shown in Scheme 2 may explain the shift in the Ni−CO region toward the end of the electrolysis, where the concentration of CO is expected to be higher. Also, such an equilibrium leads to a complex mixture of nickel species in solution considering that CO and isocyanides compete for the $\{Ni_2(dppa)_2\}$ fragment, explaining the rather large number of bands in the Ni−CO region. To determine the identity of the bands that appeared around 2000 cm^{-1}, an acetonitrile/TBAP solution of complex **2** was saturated with CO and injected into a liquid IR cell. Together with those bands, corresponding to complex **2**, new ones appeared at 2004, 1980, 1950, 1926, 1953, and 1868 cm^{-1}. No bands in the vicinity of 2138 cm^{-1}, typically for free CO, were observed.

The obvious question that follows is, do these carbonyl species show electrocatalytic activity toward CO_2? Under similar conditions, the CO dimer $[Ni_2(\mu_2\text{-dppa})_2(\mu_2\text{-CO})(CO)_2]$, synthesized according to a literature method,[5] did not show any electrocatalytic activity with respect to CO_2 reduction. This experiment offers a plausible explanation of how catalytic activity is lost during the course of electrolysis as the result of secondary reactions of the catalyst with the CO, formed by the reductive disproportionation of CO_2 to CO_3^{2-} and CO. As the electrocatalytic reaction proceeds, the number of differently substituted species having isocyanide, CO, and dppa as ligand is quite large (Scheme 2), including mononuclear and binuclear species. Some of these species may undergo similar redox processes and contribute to the electroreduction of CO_2. From the IR SEC data it is possible to quantify the amount of carbonate produced during the electrolysis (for details see Supporting Information). Assuming that the formation of one CO_3^{2-} accounts for two molecules of CO_2 reduced and that the only electrocatalytic active species is the one produced from the reduction of complex **2**, the turnover number (TON) was evaluated to be ∼40 with a turnover frequency (TOF) of ∼1.0 s^{-1}.

IR SEC in the Presence of $^{13}CO_2$. To unequivocally assign the origin of bands that appeared during CO_2 bulk electrolysis, an experiment using isotopically labeled $^{13}CO_2$ was performed. The IR SEC response is shown in Figure 5 (bottom). All bands around 2000 and 1600 cm^{-1}, previously assigned as Ni−CO and carbonate ν(CO) vibrations, were shifted toward lower energy by 43 to 46 cm^{-1} ($\nu(^{13}CO)$ 1962, 1944, 1904, 1884, 1641, 1609 cm^{-1}), very close to the theoretical value calculated from the harmonic oscillator model (45 cm^{-1}). The lower intensities for the isotopic labeled carbonate bands (1641, 1609 cm^{-1}) are more the result of poor solvent subtraction in the FT IR spectrum around 1600 cm^{-1}, because of the high molar absortivity of acetonitrile. This experiment confirms that these bands (2004, 1980, 1950, 1926, 1685, and 1650 cm^{-1}) originate from CO_2 reduction.

"Trapping" the $CO_2^{-\bullet}$ Radical. Control Experiments. It is well known that electrochemical reductions of carbon dioxide in aprotic solvents containing residual water result in formate formation. Formate results from the reaction of the anion radical $CO_2^{-\bullet}$ with a proton. The role of residual water on the electrocatalytic reaction was investigated with spectroelectrochemical reductions of CO_2-saturated acetonitrile solutions that also contained H_2O or D_2O (for spectra see Supporting Information). The spectral changes in the 2000−1600 cm^{-1} infrared region were only slightly different from those in the absence of water. When traces of H_2O are present, new bands at 1609 and 1333 cm^{-1}, assigned as formate,[25] grow in. Addition of H_2O or D_2O has no effect on those bands in the Ni−CO region, but the carbonate bands collapse, probably due to hydrogen bonding of the carbonate anion. When the solvent was dried with superacid alumina,[27,28] the formate peaks at 1609 and 1333 cm^{-1} do not appear. In our systems, we are able to reach electrochemical windows of +2 and −3.0 V with acetonitrile/TBAP solutions after purification through a column filled with previously calcinated superacid aluminum oxide. Even in this super dry solvent the catalytic activity of our system toward CO_2 remains the same, ruling out the water as the possible cause of the current enhancement observed during electrochemical reductions.

In an attempt to trap the "generated" $CO_2^{-\bullet}$ radical, large quantities of cyclohexene as a quencher (>1.5 M) in acetonitrile solution were introduced. The IR SEC shows no new bands at 1728 cm^{-1}, expected for a carboxylic acid. We conclude that these results are consistent with the single electron reduction of CO_2 to $CO_2^{\bullet-}$, but the radical anion does not appear to react as a free radical, but rather a trapped (coordinated) one.

Theoretical Calculations. Figure 6 shows the HOMO−LUMO frontier orbitals for complex **2**. The HOMO frontier molecular orbital reveals a strong contribution of metal orbitals (p_z and $d_{x^2-y^2}$) bonding to the μ-bridging isocyanide ligands and the phosphorus atoms. The d electrons are in dπ orbitals delocalized between both metals, across the conjugated bridging ligand. This orbital is bonding with respect to the Ni−C (μ-CNMe) bond, but it is a Ni−Ni antibonding orbital, with a nodal plane passing through the μ-CNMe bridge.

The plane is perpendicular to the Ni−Ni axis and bisects the molecule in two symmetrical fragments. The LUMO is further delocalized to the isocyanide phenyl rings with a small contribution from carbon and nitrogen at the terminal isocyanide ligands and having strong π^* character. This picture is supported by the

(26) Osborn, J. A.; Stanley, G. G.; Bird, P. H. *J. Am. Chem. Soc.* **1988**, *110*, 2117.

(27) Hammerich, O.; Parker, V. D. *Electrochim. Acta* **1973**, 5.

(28) Kiesele, H. *Anal. Chem.* **1981**, *53*, 1952−1954.

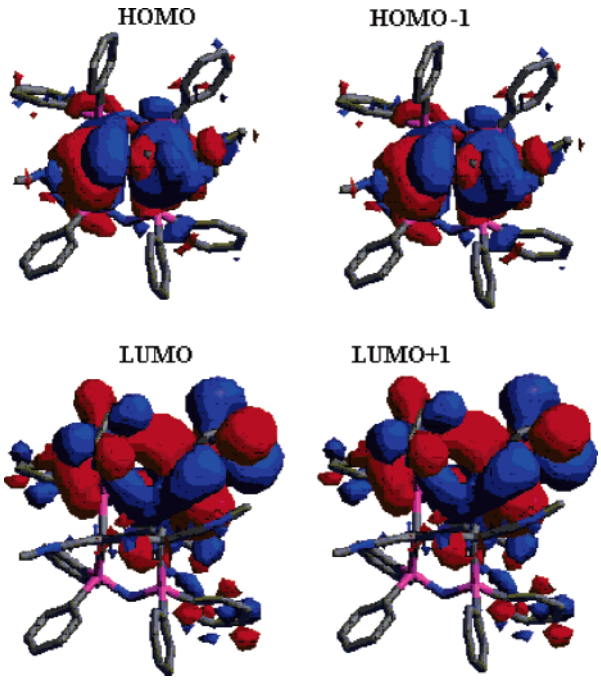

Figure 6. HOMO, HOMO^{-1}, LUMO, and LUMO^{+} orbital diagrams for complex [Ni_2(μ_2-dppa)$_3$(μ_2-CNMe)(CNMe)$_2$] (**2**) (isosurface at 0.010 au).

IR of the reduced [**2**]$^{-\bullet}$ species obtained in the SCE experiment, where ν_{CN} stretching frequencies of terminal and bridging ligands are shifted by 36 and 34 cm^{-1}, respectively, toward lower energy upon reduction. The next two orbitals below the HOMO (HOMO^{-1} and HOMO^{-2}) are close in energy and have similar symmetry (ΔE(HOMO−HOMO^{-1}) = 0.3208 eV). A similar picture is observed for the higher energy LUMO^{+1} and LUMO^{+2} orbitals (ΔE(LUMO^{+1}−LUMO) = 0.1041 eV).

Conclusions

Complexes **1**−**3** are 1 e^{-} electrocatalysts for the reduction of carbon dioxide. Reduction of the dinuclear nickel(0) complexes is largely ligand-localized, on the basis of theoretical calculations and SEC results, where the π^* orbital of the phenyl ring on the xylyl isocyanide can shuttle electrons in and out of the closed-shell d^{10}−d^{10} [Ni_2] system. The products of carbon dioxide electroreduction in the presence of complexes **1**−**3** are mainly CO and CO_3^{-2}, with small amounts of formate formed when residual water is present. Complexes **1**−**3** also react with carbon monoxide, leading to formation of carbonyl-containing species that are not active toward CO_2 reduction.

Acknowledgment. The authors wish to thank the DOE (DE-FG03-99ER14992) for support of this research. E.S.-M. thanks Dr. Brian Breedlove for his contributions to the manuscript preparation.

Supporting Information Available: Spectroscopic and electrochemical data of the complexes **1**, EPR spectra of **2**$^{-\bullet}$, and control IR SEC experiments. This material is available free of charge via the Internet at http://pubs.acs.org.

OM0494723